

# Sensitive Magnetic Rotation Spectroscopy of the OH Free Radical Fundamental Band with a Colour Centre Laser

J. Pfeiffer, D. Kirsten, P. Kalkert, and W. Urban

Institut für Angewandte Physik, Universität, Wegelerstrasse 8, D-5300 Bonn 1, Fed. Rep. Germany

Received 21 May 1981/Accepted 14 July 1981

**Abstract.** The magnetic rotation technique has been optimized and applied for spectroscopy of the OH fundamental band at about  $3670\text{ cm}^{-1}$  by use of a colour centre laser. The response of the molecules to the modulation field has been studied in detail, resulting in calculation of effective  $g$ -values, which describe the modulation sensitivity of the transitions and the phase of the signals.

**PACS:** 32,35

The production of free radicals often requires continuous flow systems and normally there is a reasonable concentration only in a definite small volume. Therefore sensitive absorption techniques are required for infra-red spectroscopy of free radicals. To enhance sensitivity special modulation techniques have to be applied. In the case of free radicals it is advantageous to use magnetic modulation, because it is selective for the paramagnetic species. "Laser magnetic resonance" is such a very sensitive technique, which utilizes the molecular Zeeman effect both to tune the absorption in resonance with the line of a laser (e.g. molecular lasers in the mid and far ir) and for effect modulation [1, 2]. However, regarding analysis of the spectra, the randomness of the required near coincidences is a serious disadvantage. This can be overcome by use of a tunable laser source and zero-field Zeeman modulation (ZM) as developed by Urban and Herrmann in connection with a spin-flip Raman laser [3]: a circularly polarized laser beam passes through an absorption cell with solenoidal coil. If a sinusoidal modulation field is applied, the beam is intensity modulated, whenever the laser tunes through a resonance of the paramagnetic species; the intensity-modulation is detected by a PSD. With the length of the absorption-path fixed, the sensitivity mainly depends on the noise of the laser.

Recently besides diode lasers and spin-flip Raman lasers colour centre lasers (CCL) are available as tunable laser sources in the infra-red. The noise of a CCL, mainly caused by the pumping ion laser, is fairly large, thus preventing sensitive spectroscopy with the ZM method. To suppress source noise Curl suggested the magnetic rotation technique (MR), which has been applied in combination with a CCL by Litfin et al. [4]. In the experimental set up a linearly polarized beam passes through the absorption cell, which is placed between two nearly crossed polarizers; if the laser is tuned through a resonance, the plane of the polarization is periodically rotated by the magnetic modulation field. This causes an intensity modulation behind the nearly crossed analyzer, which is detected by a PSD. Litfin et al. achieved a sensitivity of  $\alpha = 10^{-5}\text{ cm}^{-1}$ , with  $\alpha$  being the minimal detectable absorption coefficient.

We have optimized the method and improved the sensitivity to  $\alpha = 5 \times 10^{-7}\text{ cm}^{-1}$ . Thus we could detect a complete sequence of resonances of the OH free radical in the tuning range of our laser. The modulation sensitivity and the phase of the signals depend on the special transition and are investigated in detail. The MR method can be useful in combination with other lasers, too. With a CO laser as source a gain in sensitivity of LMR with longitudinal magnetic field

Table 1.  $g_J$ -factors and effective  $g$ -factors for modulation of the  $R$ -branch transitions of  ${}^2\Pi F_1$  OH ( $v=1\leftarrow 0$ )

$J$	$g_J$	$g_{\text{eff}}^R$
1.5	0.93	0.14
2.5	0.48	0.12
3.5	0.32	0.10
4.5	0.24	0.087
5.5	0.20	0.075

has been measured by applying the MR technique [5]. Therefore a theoretical comparison of ZM and MR method is of interest.

### 1. Effective $g$ -Factors for Magnetic Rotation

In [4] the power measured behind the analyzer in a MR set-up is calculated:

$$P = P_0/2[(1 - \cos 2\varphi) + R_A \cdot l \cdot \sin 2\varphi] \quad (1)$$

with  $P_0$  being the incident beam power,  $\varphi$  the angle of the analyzer versus the crossed position,  $l$  the length of the absorption cell and  $R_A$  twice the angle of polarization rotation per unit by the paramagnetic gas.

To derive the formula it is assumed, that the magnetic field splits the absorption line into two components of right-hand and left-hand circular polarization, respectively. They are separated by

$$\delta\omega(B) = \pm g\mu_0 B \quad (2)$$

from the line position at zero field. If  $\delta\omega(B)$  is small compared to linewidth, it holds

$$R_A = 2\omega/c \cdot dn/d\omega \cdot \delta\omega(B); \quad (3)$$

$dn/d\omega$  determines the shape of the signals,  $\delta\omega(B)$  describes the response of the transition to the modulation field. Generally an absorption line is split into more than two components by the Zeeman effect and the resulting lineshape has a more complicated form [6]. For a vibration-rotation transition  $(v'', J'', M'') \rightarrow (v', J', M')$  the Zeeman effect is described by

$$\delta\omega = \mu_0 B (M' g_{J'}^{v'} - M'' g_{J''}^{v''}) \quad (4)$$

and for the special case of  $R$ -branch transitions with  $\Delta M = \pm 1$  we get

$$\delta\omega = \mu_0 B ((M'' \pm 1) g_{J'}^{v'} - M'' g_{J''}^{v''}). \quad (5)$$

For every transition  $M'' \rightarrow M'' + 1$  there is a transition  $-M'' \rightarrow -M'' - 1$  with equal transition probability and opposite magnetic tuning behaviour. These transitions form the pairs assumed in the derivation of (1). All existing pairs contribute to the modulation signal,

partly compensating each other; to account for this, we have to replace  $\delta\omega$  or  $g$  in (2) by effective values. They can be calculated by summing up all pairs weighted by their transition probabilities, i.e.,

$$g_{\text{eff}}^R = \sum_{M''=-J''}^{J''} [(M'' + 1) g_{J'}^{v'} - M'' g_{J''}^{v''}] \cdot |\langle J'' + 1, M'' + 1 | \beta \cdot D_+ | J'', M'' \rangle|^2, \quad (6)$$

where  $D_+$  is the operator for  $\sigma^+$ -transitions, and  $\beta$  is a normalization factor chosen such that

$$\sum_{M''=-J''}^{J''} |\langle J'' + 1, M'' + 1 | \beta \cdot D_+ | J'', M'' \rangle|^2 = 1.$$

After a straightforward but lengthy calculation using the Wigner-Eckart theorem (6) transforms into

$$g_{\text{eff}}^R = g_{J'}^{v'} + (g_{J'}^{v'} - g_{J''}^{v''}) \cdot \frac{J}{2}. \quad (7a)$$

The corresponding formulae for  $Q$ - and  $P$ -branch transitions are

$$g_{\text{eff}}^Q = g_{J'}^{v'} + (g_{J''}^{v''} - g_{J'}^{v'}) \cdot \frac{1}{2}, \quad (7b)$$

$$g_{\text{eff}}^P = g_{J'}^{v'} + (g_{J''}^{v''} - g_{J'}^{v'}) \cdot \frac{J+1}{2}. \quad (7a)$$

The  $g_{\text{eff}}$ -factors determine the sensitivity to modulation and the phase of the signal of a transition. The  $g_J$ -factors of the OH free radical may be calculated using references [7, 8]. The resulting  $g_J$  and  $g_{\text{eff}}$ -factors are listed in Table 1.

### 2. Comparison Between Zeeman Modulation and Magnetic Rotation Technique

In practical cases the absorptions of free radicals will be very weak and in the magnetic rotation set-up the polarizers will be nearly crossed. The power reaching the detector as given by (1) can then be approximated by

$$P_{\text{MR}}(\varphi) = P_0 [\varphi^2 + 2 \cdot \omega/c \cdot \delta\omega_{\text{eff}}(B) \cdot dn/d\omega \cdot \varphi \cdot l]. \quad (8)$$

This has to be compared to the power falling upon the detector in a Zeeman modulation arrangement:

$$P_{\text{ZM}} = P_0 [1 - 2 \cdot \omega/c \cdot \delta\omega_{\text{eff}}(B) \cdot d\kappa/d\omega \cdot l], \quad (9)$$

where  $\kappa$  is the extinction coefficient of the absorption line. The formulae show that source noise, which is proportional to the incident power, is smaller by a factor  $\varphi^2$  in MR compared to ZM. It is apparent that the ZM signal has the shape of the derivative of the absorption curve, whereas the MR signal shows the derivative of the dispersion curve. The ZM signal

peaks at the two turning points (tp), the MR signal at the centre (c) of the absorption line.

For convenience we regard the MR signal at line centre and twice the ZM signal at the turning point as signal strength (peak-to-peak signal);  $n$  and  $\kappa$  being closely related, because they are real and imaginary part of the complex index of refraction. For purely Doppler-broadened absorption lines it is possible to evaluate the following relationship from the formula in [9]:

$$dn/d\omega|_{(c)} \approx 1.9 \cdot d\kappa/d\omega|_{(tp)}. \quad (10)$$

Using (10), the comparison of (8) and (9) shows that the signal strength in MR is reduced by about a factor  $\varphi$  compared to ZM.

This means, that MR increases the S/N-ratio on expense of the absolute signal strength. Therefore MR is especially useful in the two cases:

(a) If the laser is so powerful, that it saturates the detector, it is possible to reduce the total incident power by means of the analyzer. This reduces the signal only by the square root of the power reduction. This case occurs when using a CO laser in LMR with longitudinal magnetic field [5].

(b) If laser noise is far above detector noise (e.g. by a factor of  $10^5$  in the case of a CCL), MR is the most powerful and simple method to improve sensitivity. Nevertheless amplitude stabilization of the CCL should be applied in addition, because it increases sensitivity without decreasing absolute signal strength.

### 3. Experimental

The colour centre laser has been designed similar to that described in [10]. The crystal chamber is evacuated to  $10^{-6}$  Torr. After the formation of  $F_A$ -centres the crystal is permanently cooled to 77 K. The optical surfaces are slowly deteriorated by condensing water molecules resulting in doubling of the laser threshold after about a two-month's period. Coarse tuning is accomplished by a grating in Littrow use, fine tuning by a piezo-driven etalon. Output-coupling is done by the zeroth-order reflexion of the grating.

The resonator is completely evacuated, because even very weak, narrow-band absorptions in the resonator cause the laser to avoid the absorbed wavelength: when the resonator is tuned through the absorption, the laser oscillates just before and behind the absorption only. As water vapour in air has many, rather strong absorptions in the tuning range of the CCL, the extracavity beam path is evacuated, too. Tuning has been monitored by a 20 GHz spectrum analyzer.

To determine the optimal frequency for modulation by the Zeeman effect, the spectral distribution of laser

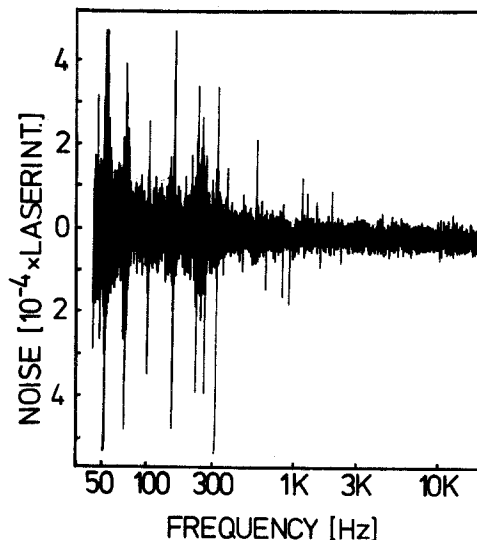


Fig. 1. Spectral distribution of relative noise amplitude of the CCL, bandwidth: 2 Hz

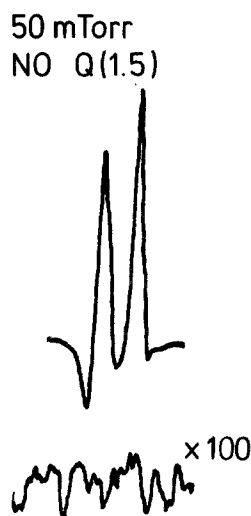


Fig. 2. MR signal from the overtone-transition  ${}^2\Pi_{3/2}(Q(1.5))$  of the NO molecule. The lower trace shows the noise 100 times amplified

noise has been measured. From Fig. 1 it is apparent that the region up to 1 kHz is not well suited for modulation, because the ripple of the krypton laser power supply and acoustic vibrations cause much noise. Beyond 1 kHz noise amplitude is reasonably low, but acoustic cross talk from the modulation coil to the laser was still found to be a problem. To avoid this we chose a modulation frequency of 7 kHz. The modulation field strength was  $\pm 550$  Gauss over a length of 20 cm.

The laser beam was polarized to a degree of  $1:5 \times 10^4$  by a grid-type polarizer, the analyzer was a  $\text{MgF}_2$  rochon prism, manufactured by Halle, Berlin, which is specified to polarize to  $1:10^5$ . A photovoltaic InSb-type detector cooled to 77 K was used. With the polarizers crossed laser noise was equal to detector noise at 1 mW incident laser power.

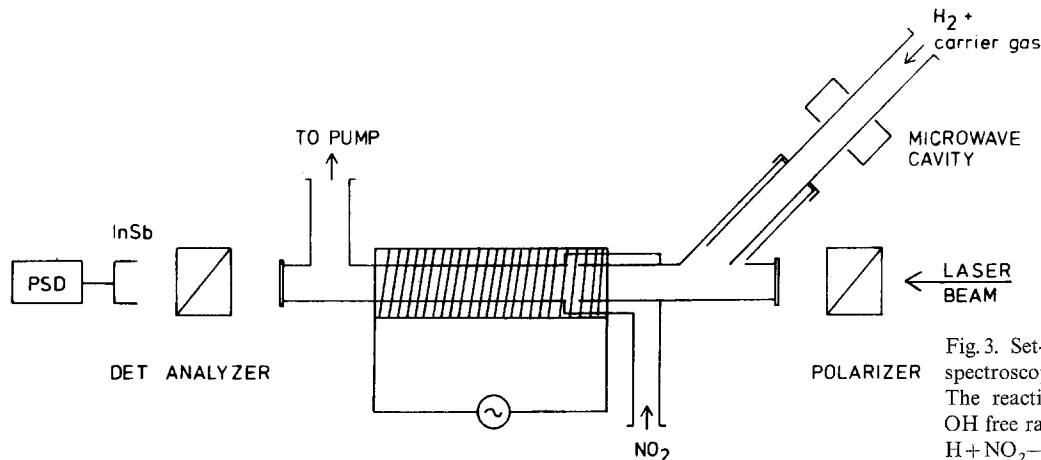


Fig. 3. Set-up for magnetic rotation spectroscopy of the OH free radical. The reaction for the production of OH free radicals is:  
 $H + NO_2 \rightarrow OH + NO$

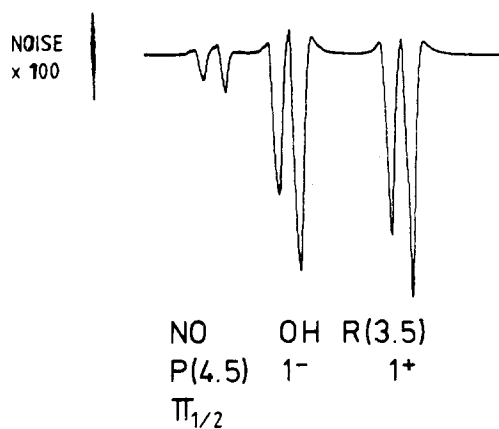


Fig. 4. MR signal from the two  $A$ -components of the fundamental transition  $R(3.5)^2\Pi F_{1\pm}$  of OH free radical. The S/N-ratio demonstrates a sensitivity of  $\sim 10^{11}$  molecules per  $cm^3$

Figure 2 shows the signal from  $NO^2\Pi_{3/2} Q(1.5)$  ( $v=2\leftarrow 0$ ). From the signal strength the minimal detectable absorption coefficient can be calculated to be  $5 \times 10^{-7} cm^{-1}$  [11].

The OH free radicals were produced by the reaction  $NO_2 + H \rightarrow OH + NO$ . The hydrogen was dissociated in a microwave discharge and the atoms were titrated with  $NO_2$  just in front of the modulated region (Fig. 3). The walls of the cell have been cleaned thoroughly with HF and left without any coating. The concentration of the OH radicals strongly depended on the purity of the cell walls. Under optimum conditions we got a signal from the  $^2\Pi F_1 R(3.5)$  OH ( $v=1\leftarrow 0$ ) transition with a S/N-ratio of 300:1 (Fig. 4). This transition has been observed by Litfin et al. [4] before. By comparison with the NO signal the concentration of

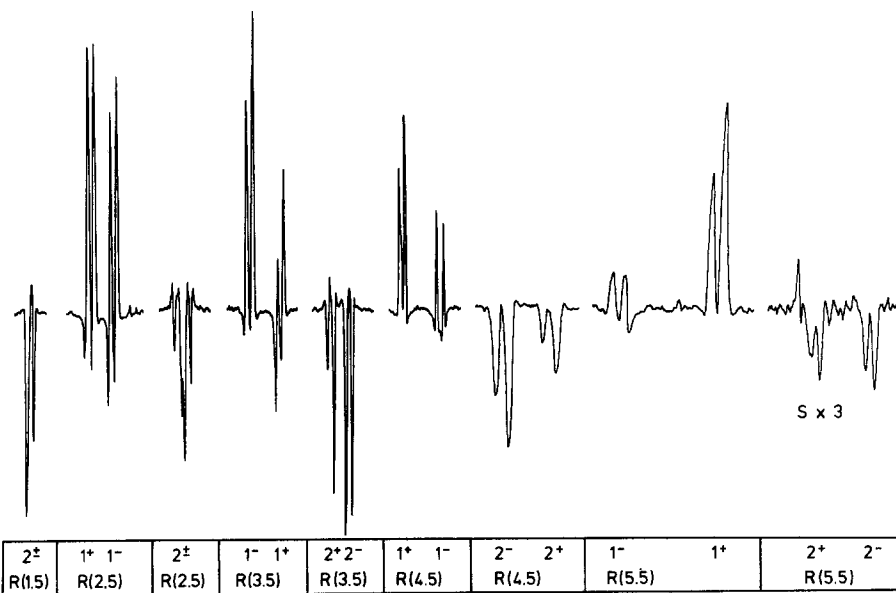


Fig. 5. Sequence of R-branch transitions of  $^2\Pi$  OH fundamental band. The phases alternate depending on the magnetic tuning behaviour of the fine-structure systems

Table 2. Wavenumbers of the observed OH transitions, taken from [12]

$R(1.5) 2\pm$	3663.73
$R(2.5) 1+$	3679.44 <sup>a</sup>
$R(2.5) 1-$	3679.59 <sup>a</sup>
$R(2.5) 2\pm$	3697.31
$R(3.5) 1-$	3708.69
$R(3.5) 1+$	3709.00
$R(3.5) 2+$	3728.48
$R(3.5) 2-$	3728.62
$R(4.5) 1+$	3736.94 <sup>a</sup>
$R(4.5) 1-$	3737.31
$R(4.5) 2-$	3757.52
$R(4.5) 2+$	3757.79
$R(5.5) 1-$	3763.90
$R(5.5) 1+$	3764.32
$R(5.5) 2+$	3784.60
$R(5.5) 2-$	3784.92

<sup>a</sup> Lines observed for the first time

OH radicals may be estimated to  $10^{13} \text{ cm}^{-3}$  on an average.

The series of OH resonances in Fig. 5 has been recorded under poorer conditions. Some of the OH transitions coincide with water absorptions and have not been recorded before. The relative phases of the signals are in agreement with the  $g_{\text{eff}}$  factors listed in Table 1. The wavenumbers in Table 2 are from [12]. At elevated power levels, necessary to get high sensitivity, the present laser system tends to operate at two hole-burning modes. This produces a pseudo doublet structure of the absorption lines. For single-mode operation the resolving power of the intracavity etalon has to be better than 2 GHz.

## Conclusions

The signals in Figs. 2, 4, and 5 have been obtained with the CCL running at 1 mW or less. A CCL is capable to produce single-mode output powers of several mW over most of the spectral region from 2.2–3.3  $\mu\text{m}$ . The sensitivity achieved with optimized MR technique makes the spectrometer suitable for free radical spectroscopy. The phases of the signals give additional information for the interpretation of the spectra obtained.

*Acknowledgements.* We wish to thank Dr. G. Litfin for the help in starting the CCL project, supplying the CC crystals and communicating results on the MR technique prior to publication. This work was supported by the “Deutsche Forschungsgemeinschaft”, partly through SFB 42.

## References

1. P.B.Davies, K.M.Evenson: In *Laser Spectroscopy*, Lecture Notes in Physics **43**, 132 (Springer, Berlin, Heidelberg, New York 1975)
2. W.Rohrbeck, A.Hinz, W.Urban: *Mol. Phys.* **41**, 925–927 (1980)
3. W.Urban, W.Herrmann: *Appl. Phys.* **17**, 325–330 (1978)
4. G.Litfin, C.R.Pollock, R.F.Curl, F.K.Tittel: *J. Chem. Phys.* **72**, 6602–6605 (1980)
5. A.Hinz: To be published
6. W.Herrmann, W.Rohrbeck, W.Urban: *Appl. Phys.* **22**, 71–75 (1980)
7. H.E.Radford: *Phys. Rev.* **122**, 114–130 (1961)
8. H.E.Radford: *Phys. Rev.* **126**, 1035–1045 (1962)
9. M.Born: *Optik* 3rd ed. (Springer, Berlin, Heidelberg, New York 1972) p. 484
10. G.Litfin, R.Beigang: *J. Phys. E.* **11**, 983–986 (1977)
11. A.S.Pine, J.W.C.Johns, A.G.Robiette: *J. Mol. Spectrosc.* **74**, 52–69 (1979)
12. J.P.Maillard, J.Chauville: *J. Mol. Spectrosc.* **63**, 120–141 (1976)